Analytical and numerical calculations of interatomic forces and stresses

X. W. Zhou [a]

[a] University of Virginia, Department of Materials Science and Engineering , 116 Engineer's
Way, Charlottesville, VA 22904-4745, USA
Published online: 19 Aug 2006.

PLEASE SCROLL DOWN FOR ARTICLE

Analytical and numerical calculations of interatomic forces and stresses

X. W. ZHOU*

Department of Materials Science and Engineering, University of Virginia, 116 Engineer's Way, Charlottesville, VA 22904 − 4745, USA

Atomistic simulation methods such as molecular dynamics require an efficient calculation of interatomic forces and stresses from pre−defined interatomic potentials. Both analytical and numerical approaches can be used to do this. Analytical approach directly calculates forces and stresses using analytical formulae, and can therefore yield accurate results. However, the force and stress expressions may become extremely complicated as the complexity level of the potential increases, resulting in a prolonged development cycle to implement new potentials. Numerical approach uses finite difference method to evaluate forces and stresses through simple calculation of energies at selected perturbations of crystal configurations. The method can be quickly implemented and tested for any potentials. However, it may result in significant numerical errors. We have compared analytical and numerical calculations of interatomic forces and stresses in molecular dynamics, and identified the conditions where numerical method can be successfully used without significant errors.

Keywords: Molecular dynamics; Interatomic potential; Semiconductors; Stress

1. Introduction

Molecular dynamics simulations have become powerful tools for analyzing assembly phenomena encountered during the vapor phase synthesis of nanostructured devices and identifying the optimized process conditions to create desired structures. These studies revealed phenomena that are difficult to see using experimental approaches, such as modulated energy deposition effects on interfaces [1], surfactant−mediated growth [2] and pin−hole formation during oxidation of ultra−thin Al layer [3].

A major time spent to develop a MD approach for simulating complicated material structures lies in the calculation of interatomic forces and stresses from a pre−defined interatomic potential. For closely packed metal systems, the embedded atom method (EAM) potential initially developed by Baskes and Daw [4] can be successfully applied [1,2,5]. EAM potentials have simple analytical equations for forces and stresses. Our recent potential model [6] combining charge transfer ionic potential (CTIP) and EAM potential has been successful to simulate the growth of amorphous AlO_x

barrier layer on a magnetic metal alloy surface [3]. However, this CTIP + EAM potential has not yet incorporated the angular dependence. As a result, it is difficult to be fitted to complex oxide crystal structures. In covalently bonded semiconductor systems such as Si, Ga and As, etc. the interactions between atoms are strongly angular dependent. Numerous angular dependent empirical potentials have been developed for these materials [7–10]. Frequently applied ones include Tersoff [9] and Stillinger−Weber [10] potentials. Unfortunately, these potentials still do not contain sufficient physical insights to allow the relative stability of a variety of phases to be correctly ordered [11].

Based upon a tight binding approximation to multi− body quantum mechanics, a theoretically reliable analytic bond−order potential (BOP) for III−V covalently bonded semiconductors has been developed and is being continuously improved [12–18]. Such a potential was found to describe well the crystal lattices and the relative order of the cohesive energies of a variety of Ga, As and GaAs phases [11]. To capture the complex surface reconstruction of GaAs surfaces, BOP needs to be combined with an electron counting

* Corresponding author. Tel.: +434-982-5672. Fax: +434-982-5677. Email: xz8n@virginia.edu

potential (ECP) [19]. While it is thought that more physics of bonding in material systems can be captured by using a BOP + CTIP + ECP potential, the complexity of the potential format becomes a significant hindrance for any practical applications. For instance, the most basic BOP that includes both σ and π bonding as well as promotion energy [17] requires a book to merely record the analytical expressions for interatomic forces and stresses derived using Mathematica software package. As a result, a direct implementation of analytical force and stress calculation, especially the validation of the code, can become a significantly prolonged process. The problem may be compounded because the potential formats need to be continuously modified during the initial development stage. A force and stress calculation approach that can be easily implemented and validated is, therefore, extremely helpful to expedite the development of the potential. If the potential formats are matured and an analytical implementation of the potential is finally preferred, then this rapid approach can also help test the analytical implementation.

A finite difference numerical method based on the calculations of energies at selected perturbations of crystal configurations can be used to evaluate interatomic forces and stresses. This approach can be implemented and tested rapidly and is almost independent of the complexity level of the potentials. However, certain numerical conditions must be satisfied before this method can produce accurate results. Here, we use literature Tersoff potential of silicon as an example to compare analytical and numerical calculations of interatomic forces and stresses. The conditions under which the numerical method can yield almost identical results to those from analytical approach are identified.

2. Analytical force expressiosns for EAM and Tersoff potentials

To examine how the analytical calculations change with the format of potentials, we first discuss the analytical force expressions derived using EAM and Tersoff potentials. In EAM, the total energy of a crystal can be calculated using [4]

$$E = \sum_{i=1}^{N} F_i(\rho_i) + \frac{1}{2} \sum_{i=1}^{N} \sum_{j=i_1}^{i_N} \varphi_{ij}(r_{ij}) \tag{1}$$

where F_i represents the embedding energy to embed an atom i into its site in the crystal where the local background electron density is ρ_i, φ_{ij} is a pair potential between atoms i and j separated by a distance r_{ij}, N is the total number of atoms in the system and i_1 and i_N are the first (1st) and the last (Nth) neighbor atoms of atom i (i.e. within a cut–off distance of the potential from

atom i. The electron density at the location of atom i, ρ_i, can be approximated as a summation of total contribution from neighboring atoms of atom i:

$$\rho_i = \sum_{j=i_1}^{i_N} a_j(r_{ij}) \tag{2}$$

where a_j refers to the electron density produced by atom j at the location of atom i. In a crystal, the three force components acting on a given atom i in the x, y and z axes arise from the energy derivatives associated with the motion of atom i in these three directions. Within EAM formulation, the motion of atom i can cause the change of embedding energy at locations of both i and j, and the change of pair energy between i and j. The force components can be easily derived as

$$f_{i_\alpha} = -\sum_{j=i_1}^{i_N} \left[\frac{\partial F_i(\rho_i)}{\partial \rho_i} \frac{\partial a_j(r_{ij})}{\partial r_{ij}} + \frac{\partial F_j(\rho_j)}{\partial \rho_j} \frac{\partial a_i(r_{ij})}{\partial r_{ij}} + \frac{\partial \varphi_{ij}(r_{ij})}{\partial r_{ij}} \right]$$
$$\times \frac{r_{i_\alpha} - r_{j_\alpha}}{r_{ij}} \tag{3}$$

where $\alpha = 1$, 2 and 3 refers to x, y and z directions, and r_{i_α} represents the α coordinate of atom i. In equation (3), the first term accounts for the embedding energy change at the location of atom i, the second term accounts for the embedding energy change at the location of atom j, and the third term arises from the pair potential energy change. Here we can see that the analytical force calculation for EAM potentials is very simple.

For Tersoff potential, the total energy of a crystal is written as [9]

$$E = \frac{1}{2} \sum_{i=1}^{N} \sum_{j=i_1}^{i_N} [V_R(r_{ij}) - B_{ij} V_A(r_{ij})] \tag{4}$$

Here, two pairwise potentials, V_R and V_A, are defined, respectively, by

$$V_R(r_{ij}) = \frac{D_{e_{ij}}}{S_{ij} - 1} \exp\left[-\beta_{ij}\sqrt{2S_{ij}}(r_{ij} - r_{e_{ij}})\right] f_c(r_{ij}) \tag{5}$$

and

$$V_A(r_{ij}) = \frac{S_{ij} D_{e_{ij}}}{S_{ij} - 1} \exp\left[-\beta_{ij}\sqrt{\frac{2}{S_{ij}}}(r_{ij} - r_{e_{ij}})\right] f_c(r_{ij}) \tag{6}$$

where D_e, S, β and r_e are species (i and j) dependent constants, and $f_c(r)$ is a cut-off smoothing function. The species dependent function B_{ij} introduces the angular dependence. B_{ij} is written as

$$B_{ij} = \left(1 + \gamma_{ij}^{n_{ij}} \xi_{ij}^{n_{ij}}\right)^{-\frac{1}{2n_{ij}}} \tag{7}$$

Here γ, n are species dependent constants, and the species dependent function ξ_{ij} is defined by

$$\xi_{ij} = \sum_{\substack{k=i_1 \\ k \neq j}}^{i_N} g_{ik}(\theta_{jik}) f_c(r_{ik}) \tag{8}$$

where θ_{jik} is the angle subtended at atom i by atoms j and k, $g_{ik}(\theta)$ is an angular dependent empirical function. $g_{ik}(\theta)$ and $f_c(r)$ are written, respectively, as

$$g_{ik}(\theta) = 1 + \frac{c_{ik}^2}{d_{ik}^2} - \frac{c_{ik}^2}{d_{ik}^2 + (h_{ik} - \cos\theta)^2} \tag{9}$$

and

$$f_c(r) = \begin{cases} 1 & r \leq r_r \\ \frac{1}{2} - \frac{1}{2}\sin\frac{\pi(2r - r_c - r_r)}{2(r_c - r_r)}, & r_r < r < r_c \\ 0, & r \geq r_c \end{cases} \tag{10}$$

Here, c, d and h are species dependent constants, r_c is the cut-off distance of the potential and r_r is the starting point for smoothing the cut-off. Parameters r_c and r_r can also be chosen to depend on the species of the pair.

If atom j or atom k is the neighbour of atom i, the motion of atom i could cause the change of B_{ij}, B_{ji} and B_{jk}. To facilitate the derivation of the force on an atom i, the crystal energy that is dependent upon the location of atom i is written as

$$E_i = \sum_{j=i_1}^{i_N} V_R(r_{ij}) - \frac{1}{2}\sum_{j=i_1}^{i_N} B_{ij} V_A(r_{ij})$$

$$- \frac{1}{2}\sum_{j=i_1}^{i_N} B_{ji} V_A(r_{ij}) - \frac{1}{2}\sum_{j=i_1}^{i_N}\sum_{\substack{k=j_1 \\ k \neq i}}^{j_N} B_{jk} V_A(r_{jk}) \tag{11}$$

In equation (11), terms are separated to distinguish different effects of B_{ij}, B_{ji} and B_{jk}. Differentiating equation (11) with respect to the position of atom i

results in the force acting on atom i, equation (12):

$$f_{i_\alpha} = -\sum_{j=i_1}^{i_N}\frac{\partial V_R(r_{ij})}{\partial r_{ij}}\frac{\partial r_{ij}}{\partial r_{i_\alpha}} - \frac{1}{4}\sum_{j=i_1}^{i_N}$$

$$\left\{ V_A(r_{ij})\left[1 + \gamma_{ij}^{n_{ij}}\left(\sum_{\substack{k=i_1 \\ k \neq j}}^{i_N} g_{ik}(\theta_{jik}) f_c(r_{ik})\right)^{n_{ij}}\right]^{-\frac{1}{2n_{ij}}-1} \cdot\right.$$

$$\times \gamma_{ij}^{n_{ij}}\left[\sum_{\substack{k=i_1 \\ k \neq j}}^{i_N} g_{ik}(\theta_{jik}) f_c(r_{ik})\right]^{n_{ij}-1} \sum_{\substack{k=i_1 \\ k \neq j}}^{i_N}\left[\frac{\partial f_c(r_{ik})}{\partial r_{ik}} g_{ik}(\theta_{jik})\frac{\partial r_{ik}}{\partial r_{i_\alpha}}\right.$$

$$\left.\left. + f_c(r_{ik})\frac{\partial g_{ik}(\theta_{jik})}{\partial\cos\theta_{jik}}\frac{\partial\cos\theta_{jik}}{\partial r_{i_\alpha}}\right]\right\} + \frac{1}{2}\sum_{j=i_1}^{i_N}$$

$$\left\{\left[1 + \gamma_{ij}^{n_{ij}}\left(\sum_{\substack{k=i_1 \\ k \neq j}}^{i_N} g_{ik}(\theta_{jik}) f_c(r_{ik})\right)^{n_{ij}}\right]^{-\frac{1}{2n_{ij}}}\frac{\partial V_A(r_{ij})}{\partial r_{ij}}\frac{\partial r_{ij}}{\partial r_{i_\alpha}}\right\}$$

$$- \frac{1}{4}\sum_{j=i_1}^{i_N}\left\{ V_A(r_{ij})\left[1 + \gamma_{ij}^{n_{ij}}\left(\sum_{\substack{k=i_1 \\ k \neq j}}^{i_N} g_{jk}(\theta_{ijk}) f_c(r_{jk})\right)^{n_{ij}}\right]^{-\frac{1}{2n_{ij}}-1}\right.$$

$$\times \gamma_{ij}^{n_{ij}}\left[\sum_{\substack{k=i_1 \\ k \neq j}}^{j_N} g_{jk}(\theta_{ijk}) f_c(r_{jk})\right]^{n_{ij}-1} \sum_{\substack{k=i_1 \\ k \neq j}}^{j_N} f_c(r_{jk})\frac{\partial g_{jk}(\theta_{ijk})}{\partial\cos\theta_{ijk}}$$

$$\left.\times\frac{\partial\cos\theta_{ijk}}{\partial r_{i_\alpha}}\right\} + \frac{1}{2}\sum_{j=i_1}^{i_N}$$

$$\left\{\left[1 + \gamma_{ij}^{n_{ij}}\left(\sum_{\substack{k=i_1 \\ k \neq j}}^{j_N} g_{jk}(\theta_{ijk}) f_c(r_{jk})\right)^{n_{ij}}\right]^{-\frac{1}{2n_{ij}}}\frac{\partial V_A(r_{ij})}{\partial r_{ij}}\frac{\partial r_{ij}}{\partial r_{i_\alpha}}\right\}$$

$$- \frac{1}{4}\sum_{j=i_1}^{i_N}\sum_{\substack{k=i_1 \\ k \neq j}}^{j_N}\left\{ V_A(r_{jk})\left[1 + \gamma_{jk}^{n_{jk}}\left(\sum_{\substack{k=i_1 \\ k \neq j}}^{j_N} g_{jl}(\theta_{kjl}) f_c(r_{jl})\right)^{n_{jk}}\right]^{-\frac{1}{2n_{jk}}-1}\cdot\right.$$

$$\times \gamma_{jk}^{n_{jk}}\left[\sum_{\substack{k=i_1 \\ k \neq j}}^{j_N} f_c(r_{jl}) g_{jl}(\theta_{kjl})\right]^{n_{jk}-1}$$

$$\left.\times\left[\frac{\partial f_c(r_{ij})}{\partial r_{ij}} g_{ji}(\theta_{ijk})\frac{\partial r_{ij}}{\partial r_{i_\alpha}} + f_c(r_{ij})\frac{\partial g_{ji}(\theta_{ijk})}{\partial\cos\theta_{ijk}}\frac{\partial\cos\theta_{ijk}}{\partial r_{i_\alpha}}\right]\right\} \tag{12}$$

In equation (12), geometric terms such as $\partial \cos\theta_{jik}/r_{i_\alpha}$ etc. can be expressed as function of atom positions. Geometric term such as $\partial \cos\theta_{jik}/r_{i_\alpha}$ and $\partial r_{ij}/r_{i_\alpha}$ are listed in Appendix. Clearly, the analytical force calculation using Tersoff potential is relatively more involving than that using EAM potential. Nevertheless, the application of equation (12) is still trivial.

3. Analytical stress expressiosns for EAM and Tersoff potentials

Similar to the previous section, we discuss the analytical stress equations for EAM and Tersoff potentials. During atomistic simulation, the size of the computational cell may be different from its equilibrium size at zero external stresses. This results in internal normal stresses for the crystal. Statically, the internal normal stresses in an α direction can be simply defined by the derivative of the crystal energy with respect to the crystal length in the same direction scaled by the area normal to that direction. However, atom vibration also contributes to the stresses due to a dynamical effect. Since we are interested in MD simulations, it is natural to incorporate this dynamical effects by introducing the stress concept from Lagrangian formalism of Newton's equation of motion.

The classical Newton's equation of motion for atom i can be expressed as

$$f_{i_\alpha} = m_i \ddot{r}_{i_\alpha} \tag{13}$$

where $\ddot{r}_{i_\alpha}$ is the second time derivative of the α coordinate of atom i, and m_i is i's mass. Equation (12) can be used in equation (13) for a simple molecular dynamics simulation. Under periodic boundary conditions with user defined periodic lengths, equation (13) can be used to solve for the atom trajectories in a fixed computational crystal cell, but cannot simulate the effects of stress, the crystal relaxation under stress and thermal expansion. In many cases such as multilayer structures, the equilibrium crystal size is not known. Then the user defined fixed periodic lengths may be far away from the equilibrium crystal sizes and fictitious stresses may be introduced. To account for stress and thermal expansion effects, the dynamic changes of periodic lengths of the crystal must also be incorporated in the equation of motion.

In classical mechanics [20], the Newton's equations of motion are defined in more general Lagrangian formalism. Assume that a system has N_F number of independent degrees of moving freedoms, $q_1, q_2, ..., q_{N_F}$. A Lagrangian L, can then be defined as the summation of the kinetic energy, K, minus the potential energy, U, of all the degrees of freedom in the system:

$$L = \sum_{i=1}^{N_F} K_{q_i} - \sum_{i=1}^{N_F} U_{q_i} \tag{14}$$

Newton's equations of motion, can then be rewritten as

$$\frac{\mathrm{d}}{\mathrm{d}t}\left(\frac{\partial L}{\partial \dot{q}_i}\right) - \frac{\partial L}{\partial q_i} = 0, \; i = 1, 2, ..., N_F \tag{15}$$

where $\dot{q}$ is time derivative of q. Equation (15) can be related to equation (13). In a free body fall case, for instance, the only degree of freedom is the height H, and L can be defined as $L = 1/2(m\dot{H}^2 - pH)$, where m and p are the mass and the weight of the free fall body, and $\dot{H}$ is the falling velocity (time derivative of H). Application of equation (15) then results in $-p = m\ddot{H}$, which is exactly equation (13). Because the degree of freedom can include both atomic positions and periodic length, equation (15) allows for the incorporation of crystal size (and the associated stresses) in the equations of motion.

Figure 1 shows a basic computational crystal cell used in simulation. Let the low bound of the cell be b_{l_α} and the high bound be b_{h_α}, then the (periodic) length of the cell in the α direction is $\lambda_\alpha = b_{h_\alpha} - b_{l_\alpha}$. The crystal volume V equals $\lambda_1\lambda_2\lambda_3$, and the equilibrium crystal volume V_0 equals $\lambda_{0_1}\lambda_{0_2}\lambda_{0_3}$, where λ_{0_α} is the equilibrium crystal length. To simplify, we take b_{l_α} as reference positions and assume them to be fixed during simulation. The change of λ_α then comes from the change of b_{h_α}. We can define scaled atomic positions s_{i_α} in the following:

$$s_{i_\alpha} = \frac{r_{i_\alpha} - b_{l_\alpha}}{\lambda_\alpha} \tag{16}$$

The effect of λ on the time derivative of s_i is negligible compared to that of r_i, and hence,

$$\dot{s}_{i_\alpha} \approx \frac{\dot{r}_{i_\alpha}}{\lambda_\alpha} \tag{17}$$
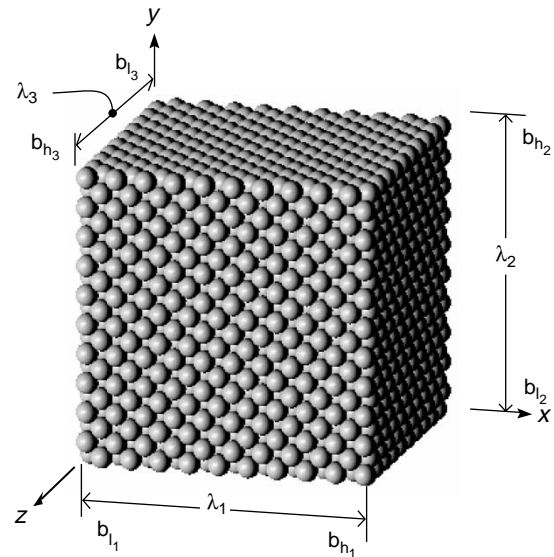

Figure 1. Computational crystal cell.

Between any two atoms i and j, we have:

$$s_{j_\alpha} - s_{i_\alpha} = \frac{r_{j_\alpha} - r_{i_\alpha}}{\lambda_\alpha} \qquad (18)$$

A Lagrangian is then defined as [21,22]

$$L = \frac{1}{2}\sum_{i=1}^{N} m_i \left[(\dot{s}_{i_1}\lambda_1)^2 + (\dot{s}_{i_2}\lambda_2)^2 + (\dot{s}_{i_3}\lambda_3)^2 \right]$$

$$- E + \frac{1}{2}\left(M_1\dot{\lambda}_1^2 + M_2\dot{\lambda}_2^2 + M_3\dot{\lambda}_3^2 \right) - P(V - V_0)$$

$$- \left[V_0(\sigma_{11} - P)\frac{\lambda_1 - \lambda_{0_1}}{\lambda_{0_1}} + V_0(\sigma_{22} - P)\frac{\lambda_2 - \lambda_{0_2}}{\lambda_{0_2}} \right.$$

$$\left. + V_0(\sigma_{33} - P)\frac{\lambda_3 - \lambda_{0_3}}{\lambda_{0_3}} \right] \qquad (19)$$

Clearly, the first term is a representation of kinetic energy of atoms, and the second term E is in fact the total potential energy of atoms [as described by equations (1) or (4)]. The third term is introduced to represent the kinetic energy associated with the change of crystal size (boundary motion), where M_α is an imaginary mass for the boundary in the α direction. The fourth term, $P(V - V_0)$, accounts for the hydrostatic energy due to a volume change under external pressure, P. The fifth term incorporates the strain energy due to a normal strain, $(\lambda_\alpha - \lambda_{0_\alpha})/\lambda_{0_\alpha}$, under the non-hydrostatic component of the stress, $(\sigma_{\alpha\alpha} - P)$ in the α direction. Here, we separately consider the effect of hydrostatic and non-hydrostatic stresses. For a given set of total normal stresses $\sigma_{\alpha\alpha}^t$, this is done by letting $P = (\sigma_{11}^t + \sigma_{22}^t + \sigma_{33}^t)/3$ and $\sigma_{\alpha\alpha} = \sigma_{\alpha\alpha}^t - P$. By using $\lambda_\alpha + \lambda_{0_\alpha} \approx 2\lambda_{0_\alpha}$, equation (19) can be simplified as

$$L = \frac{1}{2}\sum_{i=1}^{N} m_i \left[(\dot{s}_{i_1}\lambda_1)^2 + (\dot{s}_{i_2}\lambda_2)^2 + (\dot{s}_{i_3}\lambda_3)^2 \right]$$

$$- E + \frac{1}{2}\left(M_1\dot{\lambda}_1^2 + M_2\dot{\lambda}_2^2 + M_3\dot{\lambda}_3^2 \right) - P(V - V_0)$$

$$- \frac{1}{2}\left[V_0(\sigma_{11} - P)\frac{\lambda_1^2}{\lambda_{0_1}^2} \right.$$

$$\left. + V_0(\sigma_{22} - P)\frac{\lambda_2^2}{\lambda_{0_2}^2} + V_0(\sigma_{33} - P)\frac{\lambda_3^2}{\lambda_{0_3}^2} \right] \qquad (20)$$

Equation (20) contains $(3N + 3)$ independent degrees of freedom ($3N$ of s_{i_α} and 3 of λ_α). Operation of equation (15) on equation (20) with respect to s_{i_α} results in the first set of $3N$ equations of motion:

$$m_i\ddot{s}_{i_\alpha} = \frac{f_{i_\alpha} - 2m_i\dot{\lambda}_\alpha\dot{s}_{i_\alpha}}{\lambda_\alpha}, \quad i = 1,2,\ldots,N, \quad \alpha = 1,2,3 \quad (21)$$

Operation of equation (15) on equation (20) with respect to λ_α yields second set of 3 equations:

$$M_\alpha\ddot{\lambda}_\alpha = (\Phi_{\alpha\alpha} - P)\frac{V}{\lambda_\alpha} - \frac{(\sigma_{\alpha\alpha} - P)V_0\lambda_\alpha}{\lambda_{0_\alpha}^2}, \quad \alpha = 1,2,3 \quad (22)$$

where

$$\Phi_{\alpha\alpha} = -\frac{\lambda_\alpha}{V}\frac{\partial E}{\partial \lambda_\alpha} + \frac{\lambda_\alpha^2}{V}\sum_{i=1}^{N} m_i\dot{s}_{i_\alpha}^2, \quad \alpha = 1,2,3 \qquad (23)$$

Equations (21) and (22) define the equations of motion for MD simulations under flexible periodic length conditions. They also define the internal stresses $\Phi_{\alpha\alpha}$. Clearly the first term in equation (23) is exactly the static stresses ($\Phi_{\alpha\alpha}^s$), and the second term can be viewed as dynamical stresses ($\Phi_{\alpha\alpha}^d$). $\Phi_{\alpha\alpha}$ can balance the external normal stress $\sigma_{\sigma\sigma}$ to achieve equilibrium. Using equation (1) or (4), $\Phi_{\alpha\alpha}$ can be expressed as

$$\Phi_{\alpha\alpha} = \sum_{i=1}^{N} \phi_{i_{\alpha\alpha}} \qquad (24)$$

where for EAM potential

$$\phi_{i_{\alpha\alpha}} = \frac{\lambda_\alpha}{V}\left[-\frac{\partial F_i(\rho_i)}{\partial \lambda_\alpha} - \frac{1}{2}\sum_{j=i_1}^{i_N} \frac{\partial \varphi_{ij}(r_{ij})}{\partial \lambda_\alpha} + m_i\dot{s}_{i_\alpha}^2\lambda_\alpha \right],$$

$$\alpha = 1,2,3 \qquad (25)$$

and for Tersoff potential

$$\phi_{i_{\alpha\alpha}} = \frac{\lambda_\alpha}{V}\left\{ -\frac{1}{2}\sum_{j=i_1}^{i_N} \frac{\partial \left[V_R(r_{ij}) - B_{ij}V_A(r_{ij}) \right]}{\partial \lambda_\alpha} + m_i\dot{s}_{i_\alpha}^2\lambda_\alpha \right\},$$

$$\alpha = 1,2,3 \qquad (26)$$

The values of $\phi_{i_{\alpha\alpha}}$ are associated with individual atom i. Because summation of $\phi_{i_{\alpha\alpha}}$ over all atoms gives the total internal stresses, $\phi_{i_{\alpha\alpha}}$ can be viewed as the "atomic stresses".

Dynamical stresses can be easily calculated. In order to apply equations (22) and (23), one needs analytical expressions for static stress $\Phi_{\alpha\alpha}^s$. For EAM potential, we got

$$\Phi_{\alpha\alpha}^s = -\frac{\lambda_\alpha}{V}\frac{\partial E}{\partial \lambda_\alpha} = -\frac{\lambda_\alpha}{V}\sum_{i=1}^{N}$$

$$\left[\frac{\partial F_i(\rho_i)}{\partial \rho_i}\sum_{j=i_1}^{i_N} \frac{\partial a_j(r_{ij})}{\partial r_{ij}}\frac{\partial r_{ij}}{\partial \lambda_\alpha} + \frac{1}{2}\sum_{j=i_1}^{i_N} \frac{\partial \varphi_{ij}(r_{ij})}{\partial r_{ij}}\frac{\partial r_{ij}}{\partial \lambda_\alpha} \right] \qquad (27)$$

and for Tersoff potential, we derived

$$\Phi^s_{\alpha\alpha} = -\frac{\lambda_\alpha}{V}\frac{\partial E}{\partial \lambda_\alpha} = -\frac{\lambda_\alpha}{2V}\sum_{i=1}^{N}\sum_{j=i_1}^{i_N}$$

$$\left[\frac{\partial V_R(r_{ij})}{\partial r_{ij}} - B_{ij}\frac{\partial V_A(r_{ij})}{\partial r_{ij}}\right]\frac{\partial r_{ij}}{\partial \lambda_\alpha}$$

$$-\frac{\lambda_\alpha}{4V}\sum_{i=1}^{N}\sum_{j=i_1}^{i_N}V_A(r_{ij})\left(1+\gamma_{ij}^{n_{ij}}\xi_{ij}^{n_{ij}}\right)^{-\frac{1}{2n_{ij}}-1}\gamma_{ij}^{n_{ij}}\xi_{ij}^{n_{ij}-1}$$

$$\times\sum_{\substack{k=i_1\\k\neq j}}^{i_N}\left[\frac{\partial f_c(r_{ik})}{\partial r_{ik}}g_{ik}(\theta_{jik})\frac{\partial r_{ik}}{\partial \lambda_\alpha}\right.$$

$$\left.+f_c(r_{ik})\frac{\partial g_{ik}(\theta_{jik})}{\partial\cos\theta_{jik}}\frac{\partial\cos\theta_{jik}}{\partial\lambda_\alpha}\right] \quad (28)$$

Again, the geometric terms such as $\partial\cos\theta_{jik}/\lambda_\alpha$ and $\partial r_{ij}/\lambda_\alpha$ in equations (27) and (28) are listed in the Appendix. Both equations (27) and (28) can be easily applied. By using the equations provided above and in the Appendix, the $(3N+3)$ equations of motion, equations (21) and (22), can be easily solved to get s_{i_α} [which can be converted to r_{i_α} using equation (16)] and λ_α, both as a function of time.

For pair potential composed only of φ_{ij}, if the dynamical part is ignored (i.e. assuming 0 K), then the microscopic internal stress is reduced to

$$\sum_{i=1}^{N}\phi_{i_{\alpha\alpha}} = -\frac{1}{2V}\sum_{i=1}^{N}\sum_{j=i_1}^{i_N}\left[\frac{\partial\varphi_{ij}(r_{ij})}{\partial r_{ij}}\frac{(r_{j_\alpha}-r_{i_\alpha})^2}{r_{ij}}\right] \quad (29)$$

This is the well known formula for the stress [23]. In this simple case, we can also write

$$f_{j,i_\alpha} = -\frac{\partial\varphi_{ij}(r_{ij})}{\partial r_{ij}}\frac{r_{i_\alpha}-r_{j_\alpha}}{r_{ij}} \quad (30)$$

where f_{j,i_α} represents the α component of the force exerted on atom i by atom j. Substituting equation (30) into equation (29), we have:

$$\sum_{i=1}^{N}\phi_{i_{\alpha\alpha}} = -\frac{1}{2V}\sum_{i=1}^{N}\sum_{j=i_1}^{i_N}\left[f_{j,i_\alpha}(r_{j_\alpha}-r_{i_\alpha})\right] \quad (31)$$

It appears that equation (31) can be further simplified as:

$$\sum_{i=1}^{N}\phi_{i_{\alpha\alpha}} = \frac{1}{2V}\left(\sum_{j=1}^{N}\sum_{i=j_1}^{j_N}f_{i,j_\alpha}r_{j_\alpha} + \sum_{i=1}^{N}\sum_{j=i_1}^{i_N}f_{j,i_\alpha}r_{i_\alpha}\right)$$

$$= \frac{1}{V}\sum_{i=1}^{N}f_{i_\alpha}r_{i_\alpha} \quad (32)$$

However, because $f_{i_\alpha} = 0$ at equilibrium, equation (32) predicts that any equilibrium states would have zero stress, which is not true when a crystal is equilibrated under the condition where the periodic lengths of the computational cell deviate from their equilibrium counterparts. Obviously, equation (32) is valid using free boundary conditions where stresses always relax to zero as long as forces relax to zero. Under periodic boundary conditions where the same atoms may fall in different cells, only relative value such as $r_{j_\alpha} - r_{i_\alpha}$ is definite, and the absolute value such as r_{i_α} is not definite. As a result, the operation performed in equation (32) is not valid for such periodic boundary conditions. This explains why only equation (31), but not equation (32), can be used to calculate stresses.

4. Numerical force and stress expressions

Forces and static stresses can be calculated numerically using a central finite difference method. To calculate forces on an atom i, the crystal energy is viewed as a function of its coordinates $E_i = E_i(\ldots, r_{i_1}, r_{i_2}, r_{i_3}, \ldots)$. A small finite step length Δr is defined. The α coordinate of atom i is, respectively, displaced by $-\Delta r$ and Δr. The α component of the force acting on atom i can then be evaluated using:

$$f_{i_\alpha} = -\frac{E_i(\ldots, r_{i_\alpha}+\Delta r, \ldots) - E_i(\ldots, r_{i_\alpha}-\Delta r, \ldots)}{\Delta r} \quad (33)$$

Similarly, to calculate stresses, the crystal energy is viewed as a function of crystal lengths $E_\lambda = E_\lambda(\ldots, \lambda_1, \lambda_2, \lambda_3, \ldots)$. A small step length $\Delta\lambda$ is defined. The α-th periodic length is incremented by $-\Delta\lambda$ and $\Delta\lambda$, respectively. The static stress $\Phi^s_{\alpha\alpha}$ is then approximated by

$$\Phi^s_{\alpha\alpha} =$$

$$-\frac{\lambda_\alpha}{V}\frac{E_\lambda(\ldots, \lambda_\alpha+\Delta\lambda, \ldots) - E_\lambda(\ldots, \lambda_\alpha-\Delta\lambda, \ldots)}{\Delta\lambda} \quad (34)$$

Equations (33) and (34) are very simple, and are general to any potentials. However, the values of Δr and $\Delta\lambda$ need to be very small for equations (33) and (34) to approach analytical expressions. Because Δr and $\Delta\lambda$ are in the denominator, this could cause significant numerical errors and the failure of the method. The question is if an appropriate set of Δr and $\Delta\lambda$ exists so that the numerical calculations can approach the results of analytical calculations, and what the appropriate values for Δr and $\Delta\lambda$ are.

5. Analytical and numerical calculations of interatomic forces and stresses

As an example, the literature Tersoff potential of Si [9] was used to compare the analytical and numerical calculations of forces and stresses. The parameters of the potential are listed in table 1.

Table 1. Tersoff parameters for Si potential.

$D_e(eV)$	S	$\beta(\mathring{A}^{-1})$	$r_e(\mathring{A})$	γ	n	c	d	h	$r_r(\mathring{A})$	$r_c(\mathring{A})$
2.66606	1.43165	1.46555	2.29516	1.1×10^{-6}	0.78734	100390	16.217	−0.59825	2.7	3.0

A diamond cubic bulk silicon crystal containing 16 ($40\bar{4}$) planes in the *x* direction, 24 (040) planes in the *y* direction and 16(404) planes in the *z* direction was used for the calculations under the periodic boundary conditions in all three directions. The crystal had a total number of 1536 atoms. It was initially created by assigning atom coordinates to equilibrium lattice sites, and was then further relaxed under flexible periodic length conditions using an energy minimization process. To evaluate results under stress states and random perturbation of atom positions, the crystal was first uniformly stretched by a strain of 0.005 and then equilibrated using MD simulations under fixed periodic length conditions at a temperature of 1000 K for 10 ps. With this crystal, all force components acting on each of the atoms and the three normal stresses were calculated using the analytical method, equations (12) and (28), and the numerical method, equations (33) and (34). For the analytical method, we used single precision variables in the code. Both single and double precision variables were used for the numerical calculations where the numerical error can become a serious problem. Numerical calculations were performed at various step lengths Δr and $\Delta\lambda$. The same set of calculations was repeated several times with the initial atom velocities created using different random number seeds.

A standard deviation (from the analytical calculations) can be used to quantify the errors of the numerical calculations. The standard deviation for a given force component calculated using the numerical method from that calculated using the analytical method is defined as

$$\sigma_\alpha = \sqrt{\frac{\sum_{i=1}^{N}(f_{i_\alpha}^f - f_{i_\alpha}^a)^2}{N}} \qquad (35)$$

where $f_{i_\alpha}^f$ and $f_{i_\alpha}^a$ are the force component calculated using the finite difference and analytical methods, respectively. The average magnitude of the force is calculated as

$$\bar{f}_\alpha = \frac{\sum_{i=1}^{N}|f_{i_\alpha}^a|}{N} \qquad (36)$$

The results of $\sigma_\alpha/\bar{f}_\alpha$ ratio as a function of step length Δr are shown in figures 2(a)–(c) for the *x*, *y* and *z* directions ($\alpha = 1, 2, 3$). In figure 2, the five solid lines represent five separate calculations using double precision variables, and the five thin dash lines refer to five separate calculations using single precision variables. Different calculations provide convincing conclusion for the effects of the step length on the errors for the numerical calculations of all force components. For the single precision calculations, the errors decrease as the step length is decreased from 0.2 to about 0.05 Å. However, a further decrease in the step length causes a sharp increase in the errors. This is because single precision variables cannot sense the small change of energy associated with a small change of step length, and hence result in significant numerical errors. It can be seen that the least errors that can be achieved by single precision calculations is around 0.03 at a step length

between 0.04 and 0.08 Å. Obviously, single precision finite difference method cannot be satisfactorily used for the MD simulations.

For the double precision calculations, all the calculations show that the errors are continuously reduced when the step length is reduced. At a step length around 0.001 Å, the results obtained from the numerical method is almost indistinguishable from those obtained from the analytical method. Also, it is noticed that single and double precision calculations merge at large step lengths, indicating the point where the energy change caused by a large step length starts to be sensed by single precision variables.

Fractional deviation for a stress component calculated using the numerical method from that calculated using the
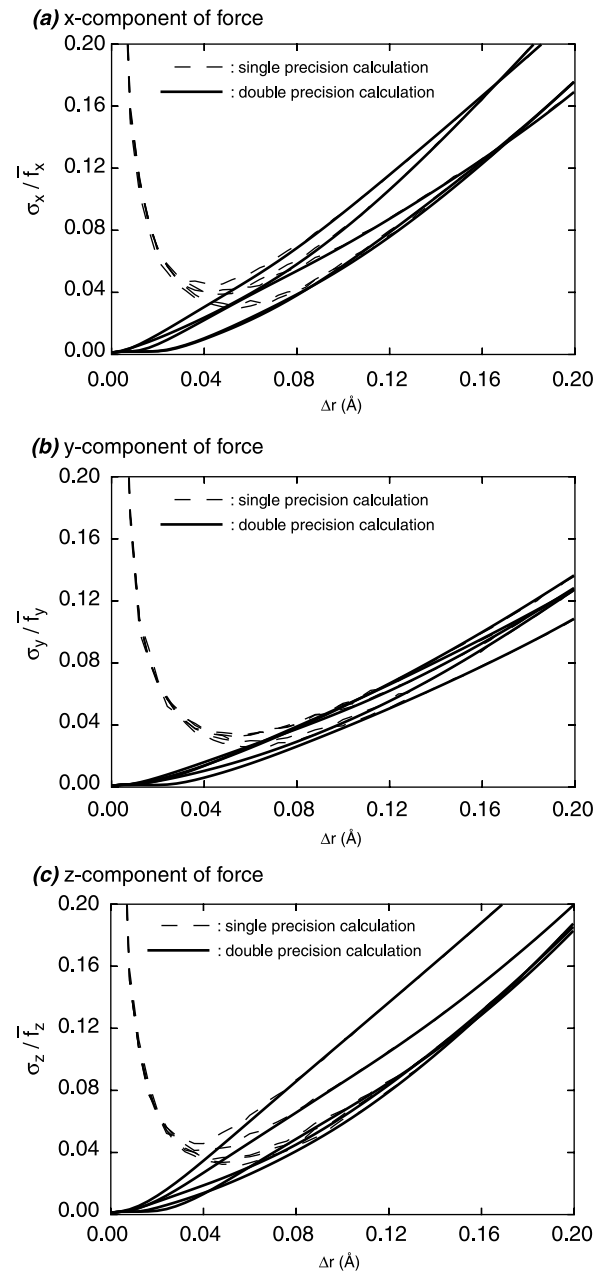

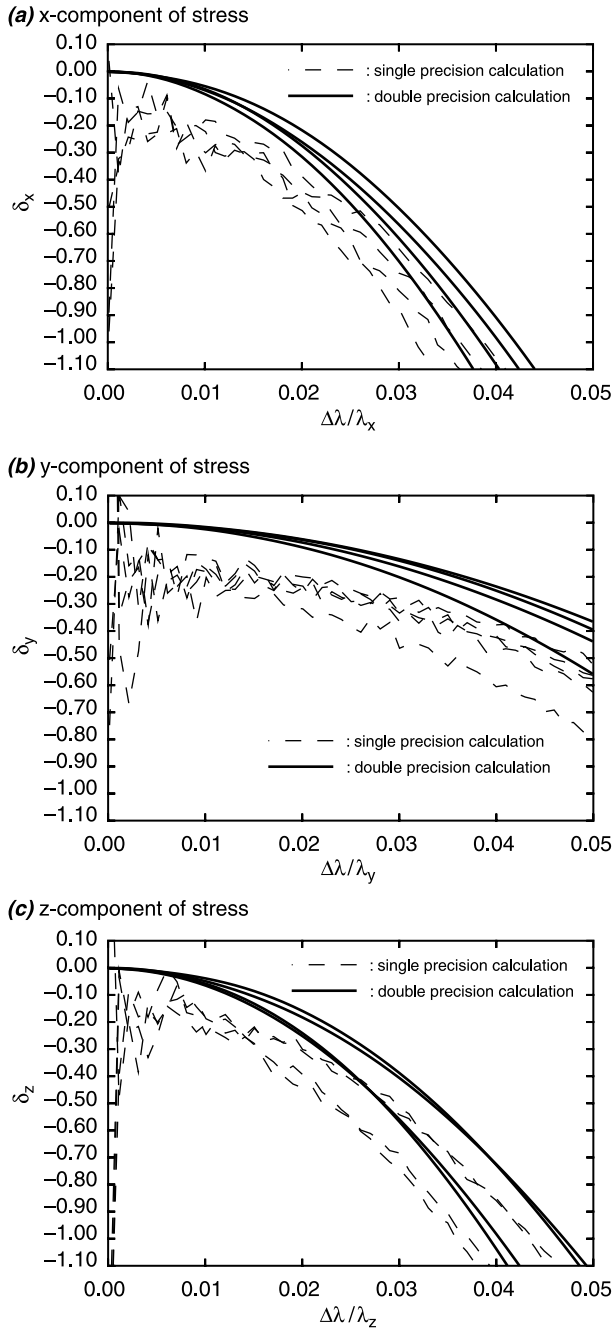Figure 2. Force deviation as a function of step length.

(a) x-component of stress

(b) y-component of stress

(c) z-component of stress

Figure 3. Stress deviation as a function of step length.

analytical method is defined as

$$\delta_\alpha = \frac{\Phi_{\alpha\alpha}^{s,f} - \Phi_{\alpha\alpha}^{s,a}}{\Phi_{\alpha\alpha}^{s,a}} \qquad (37)$$

where $\Phi_{\alpha\alpha}^{s,f}$ and $\Phi_{\alpha\alpha}^{s,a}$ refer to the values of $\Phi_{\alpha\alpha}^{s}$ calculated using the finite difference and the analytical methods, respectively. The results of δ_α as a function of fractional step length $\Delta\lambda/\lambda_\alpha$ are shown in figures 3(a)–(c) for the x, y and z directions. Here, the four solid lines represent four separate calculations using double precision variables, and the four thin dash lines refer to four separate calculations using single precision variables. Figure 3 indicates that for

the single precision calculations, the errors are relatively smoothly reduced as the fractional step length is reduced from 0.05 to about 0.02. However, when the fractional step length is below 0.02, the data become noisy, and big numerical errors can occur. For the entire step length regime, no satisfactory results can be obtained for the single precision calculations. Contrarily, the errors for the double precision calculation are continuously reduced when the step length is reduced. At a fractional step length of about 0.001, all calculations show negligible errors for the numerical method.

6. Conclusions

The analytical calculations of interatomic forces and stresses in MD simulations rely on the form of particular interatomic potential, and sometimes can be complicated and require prolonged developing efforts. A numerical method can be alternatively used. The numerical method is simple to implement, and is general to any potentials. It offers a rapid prototyping approach for both developing new potentials and testing analytical implementations. Our detailed studies indicated that such an approach was successful when double precision variables were used; the step length for force calculation was around 0.001 Å; and the fractional step length for stress calculation was around 0.001.

Appendix

If r_{i_α}, r_{j_α} and r_{k_α} represent coordinates of atoms i, j and k in the α direction, then the spacing between any two atoms i and j is

$$r_{ij} = \sqrt{(r_{j_1} - r_{i_1})^2 + (r_{j_2} - r_{i_2})^2 + (r_{j_3} - r_{i_3})^2} \qquad (A1)$$

and the angle subtended at atom i by atoms j and k, θ_{jik}, can be defined by

$$\cos\theta_{jik}$$
$$= \frac{(r_{j_1} - r_{i_1})(r_{k_1} - r_{i_1}) + (r_{j_2} - r_{i_2})(r_{k_2} - r_{i_2}) + (r_{j_3} - r_{i_3})(r_{k_3} - r_{i_3})}{r_{ij} r_{ik}} \qquad (A2)$$

It is then easy to derive

$$\frac{\partial r_{ij}}{\partial r_{i_\alpha}} = \frac{r_{i_\alpha} - r_{j_\alpha}}{r_{ij}} \qquad (A3)$$

$$\frac{\partial\cos\theta_{jik}}{\partial r_{i_\alpha}}$$
$$= \frac{(2r_{i_\alpha} - r_{j_\alpha} - r_{k_\alpha})r_{ij}r_{ik} - \cos\theta_{jik}\left[(r_{i_\alpha} - r_{k_\alpha})r_{ij}^2 + (r_{i_\alpha} - r_{j_\alpha})r_{ik}^2\right]}{r_{ij}^2 r_{ik}^2} \qquad (A4)$$

$$\frac{\partial\cos\theta_{jik}}{\partial r_{j_\alpha}} = \frac{(r_{k_\alpha} - r_{i_\alpha})r_{ij} - \cos\theta_{jik} \cdot r_{ik}(r_{j_\alpha} - r_{i_\alpha})}{r_{ij}^2 r_{ik}} \qquad (A5)$$

and

$$\frac{\partial \cos\theta_{jik}}{\partial r_{k_\alpha}} = \frac{(r_{j_\alpha} - r_{i_\alpha})r_{ik} - \cos\theta_{jik} \cdot r_{ij}(r_{k_\alpha} - r_{i_\alpha})}{r_{ij}r_{ik}^2} \tag{A6}$$

Using equation (18), it is also easy to derive:

$$\frac{\partial r_{ij}}{\partial \lambda_\alpha} = \frac{\partial r_{ij}}{\partial (r_{j_\alpha} - r_{i_\alpha})}\frac{\partial (r_{j_\alpha} - r_{i_\alpha})}{\partial \lambda_\alpha} = \frac{(r_{j_\alpha} - r_{i_\alpha})^2}{r_{ij}}\frac{1}{\lambda_\alpha} \tag{A7}$$

and

$$\frac{\partial \cos\theta_{jik}}{\partial \lambda_\alpha} = \frac{\partial \cos\theta_{jik}}{\partial (r_{j_\alpha} - r_{i_\alpha})}\frac{\partial (r_{j_\alpha} - r_{i_\alpha})}{\partial \lambda_\alpha}$$

$$+ \frac{\partial \cos\theta_{jik}}{\partial (r_{k_\alpha} - r_{i_\alpha})}\frac{\partial (r_{k_\alpha} - r_{i_\alpha})}{\partial \lambda_\alpha}$$

$$= \frac{2(r_{j_\alpha} - r_{i_\alpha})(r_{k_\alpha} - r_{i_\alpha})r_{ij}r_{ik} - \cos\theta_{jik}\left[r_{ij}^2(r_{k_\alpha} - r_{i_\alpha})^2 + r_{ik}^2(r_{j_\alpha} - r_{i_\alpha})^2\right]}{r_{ij}^2 r_{ik}^2 \lambda_\alpha} \tag{A8}$$

References

[1] X.W. Zhou, H.N.G. Wadley, R.A. Johnson, D.J. Larson, N. Tabat, A. Cerezo, A.K. Petford-Long, G.D.W. Smith, P.H. Clifton, R.L. Martens, T.F. Kelly. Atomic scale structure of sputtered metal multilayers. *Acta Mater.*, **49**, 4005 (2001).

[2] W. Zou, H.N.G. Wadley, X.W. Zhou, R.A. Johnson. Surfactant-mediated growth of giant magnetoresistance multilayers. *Phys. Rev. B*, **64**, 174418 (2001).

[3] X.W. Zhou, H.N.G. Wadley. Atomistic simulation of AlO$_x$ magnetic tunnel junction growth. *Phys. Rev. B*, **71**, 54418 (2005).

[4] M.S. Daw, M.I. Baskes. Embedded-Atom method: derivation and application to impurities, surfaces, and other defects in metals. *Phys. Rev. B*, **29**, 6443 (1984).

[5] X.W. Zhou, H.N.G. Wadley. Atomistic simulations of the vapor deposition of Ni/Cu/Ni multilayers: the effects of adatom incident energy. *J. Appl. Phys.*, **84**, 2301 (1998).

[6] X.W. Zhou, H.N.G. Wadley, J.S. Filhol, M.N. Neurock. Modified charge transfer-embedded atom method potential for Metal/Metal oxide systems. *Phys. Rev. B*, **69**, 35402 (2004).

[7] J.F. Justo, M.Z. Bazant, E. Kaxiras, V.V. Bulatov, S. Yip. Interatomic potential for silicon defects and disordered phases. *Phys. Rev. B*, **58**, 2539 (1998).

[8] S. Erkoc, T. Halicioglu, W.A. Tiller. Simulation calculations for gold clusters on the GaAs(110) surface. *Surf. Sci.*, **274**, 359 (1992).

[9] J. Tersoff. Modeling solid-state chemistry: interatomic potentials for multicomponent syetems. *Phys. Rev. B*, **39**, 5566 (1989).

[10] F.H. Stillinger, T. A. Weber. Computer simulation of local order in condensed phases of silicon. *Phys. Rev. B*, **31**, 5262 (1985).

[11] D.A. Murdick, X.W. Zhou, H.N.G. Wadley. An assessment of interatomic potentials for molecular dynamis simulations of GaAs deposition, to be published.

[12] D.G. Pettifor. New many-body potential for the bond order. *Phys. Rev. Lett.*, **63**, 2480 (1989).

[13] D.G. Pettifor, I. I. Oleinik. Analytic bond-order potentials beyond Tersoff-Brenner. I. Theory. *Phys. Rev. B*, **59**, 8487 (1999).

[14] I.I. Oleinik, D.G. Pettifor. Analytic bond-order potentials beyond Tersoff-Brenner. II. Application to the hydrocarbons. *Phys. Rev. B*, **59**, 8500 (1999).

[15] D.G. Pettifor, I.I. Oleinik. Bounded analytic bond-order potentials for σ and π bonds. *Phys. Rev. Lett.*, **84**, 4124 (2000).

[16] D.G. Pettifor, I.I. Oleinik. Analytic bond-order potential for open and close-packed phases. *Phys. Rev. B*, **65**, 172103 (2002).

[17] D.G. Pettifor, M.W. Finnis, D. Nguyen-Manh, D.A. Murdick, X.W. Zhou, H.N.G. Wadley. Analytic bond-order potentials for multi-component systems. *Mater. Sci. Eng. A*, **365**, 2 (2004).

[18] R. Drautz, D. Nguyen-Manh, D.A. Murdick, X.W. Zhou, H.N.G. Wadley, D. G. Pettifor. Interatomic bond-order potentials and cluster expansions. *TMS Lett.*, **1**, 31 (2004).

[19] X.W. Zhou, D.A. Murdick, H.N.G. Wadley. An electron counting modification to potentials for covalently bonded surfaces, to be published.

[20] H. Goldstein. *Classical Mechanics*, p. 215, Addison-Wesley Publishing Company, Inc. (1965).

[21] H.C. Anderson. Molecular dynamics simulations at constant pressure and/or temperature. *J. Chem. Phys.*, **72**, 2384 (1980).

[22] J.R. Ray, A. Rahman. Statistical ensembles and molecular dynamics studies of anisotropic solids. *J. Chem. Phys.*, **80**, 4423 (1984).

[23] Z.S. Basinski, M.S. Duesbery, R. Taylor. *Interatomic Potentials and Simulation of Lattice Defects, Battelle Colloquium*, P.C. Gehlen, J.R. Beeler, Jr., R.I. Jaffee (Eds.), p. 537, Plenum Press, New York (1971).